

Fine structure and spin dynamics of excitons in the GaAs/Al_xGa_{1-x}As superlatticesI. Ya. Gerlovin,^{*} Yu. K. Dolgikh, S. A. Eliseev, and V. V. Ovsyankin
*Vavilov State Optical Institute, St.-Petersburg 199034, Russia*Yu. P. Efimov and V. V. Petrov
*Institute of Physics, St.-Petersburg State University, St.-Petersburg 198504, Russia*I. V. Ignatiev and I. E. Kozin
*Masumoto Single Quantum Dot Project, ERATO, JST, Japan and Institute of Physics, St.-Petersburg State University, St.-Petersburg 198504, Russia*Y. Masumoto
Masumoto Single Quantum Dot Project, ERATO, JST, Japan and Institute of Physics, University of Tsukuba, Tsukuba 305-8571, Japan
(Received 3 July 2001; published 26 December 2001)

Picosecond kinetics of polarized resonant photoluminescence (PL) of HH excitons in the GaAs/AlGaAs superlattices is studied in an external magnetic field. The measurements were made in real time using a streak camera. For the magnetic field aligned along the heterostructure growth direction, the resonant PL exhibits oscillations in the degree of linear polarization. The oscillations are ascribed to quantum beats between sublevels of the optically active excitonic doublet split by the magnetic field. For the magnetic field aligned along the plane of the layers, the resonant PL is found to exhibit oscillations in circular polarization. These oscillations are related to beats between states of the optically active and optically inactive excitonic doublets. Experimental dependence of the oscillation frequency on the magnetic field strength and orientation has allowed us to determine the hole and electron g factors and the electron-hole exchange energy. Dynamics of the degree of circular polarization of the PL in magnetic field is used to measure the energy relaxation rate of the exciton spin states. In the magnetic field exceeding 1 T, the energy relaxation rate is shown to be magnetic-field independent and equal $(1 \pm 0.2) \times 10^{10} \text{ s}^{-1}$. This value is found to be much smaller than the spin phase relaxation rate determined from decay of the quantum beats in linear polarization. Unlike the energy relaxation rate, the latter grows linearly with the field strength and equals $(5 \pm 0.5) \times 10^{10} \text{ s}^{-1}$ at 5 T. It is concluded that the main mechanism responsible for loss of macroscopic spin coherence is the reversible dephasing within inhomogeneously broadened system.

DOI: 10.1103/PhysRevB.65.035317

PACS number(s): 78.47.+p, 67.57.Lm, 71.35.-y, 71.70.Ej

I. INTRODUCTION

Spin states of free carriers in the high-quality GaAs-based heterostructures reveal high stability—the spin relaxation times of electrons and holes can reach hundreds of picoseconds or even units of nanoseconds.^{1,2} The spin relaxation times of the electron-hole pairs coupled by Coulomb interaction (excitons) appear to be much shorter. Polarization experiments performed using ultrafast matrix scanning system (streak camera)³ and two-pulse methods (four-wave mixing,⁴ up-conversion of excitonic luminescence,^{5,6} and photoinduced birefringence⁷) yielded similar results. According to these results, the exciton spin relaxation time in favorable conditions (low temperature and low excitation power density) may lie in the range of several tens of picoseconds. At the same time, the question about what particular process controls the relaxation times measured in such experiments remains open. As the main processes of the relaxation over spin sublevels are considered either independent flips of the electron or hole spins,⁴ or appropriated flip of the exciton spin as a whole,^{6,7} Dynamics of polarization characteristics of the exciton emission is affected not only by the energy (population) relaxation but also by dephasing leading to destruction of coherence of the exciton spin states.⁸ The pre-

dominant process of the exciton spin relaxation in quasi-two dimensional (2D) epitaxial heterostructures is not established so far.

In the papers cited above, the measurements were made either in the absence of external fields,³⁻⁶ when splitting of the fine-structure sublevels has a random nature, or with the use of only one type of the light polarization (either circular⁹ or linear⁷). At the same time, to reliably distinguish between the phase and energy relaxation processes, one has to realize a situation when polarization characteristics of each sublevel of the fine structure appear to be fairly definite. In this case, by choosing a proper polarization of the excitation, one can either populate pure states and follow the population relaxation or excite a coherent superposition of several sublevels and measure the rate of dephasing leading to the coherence decay. This is the approach we used in this paper.

We studied picosecond dynamics of the linear and circular polarized resonant photoluminescence of HH excitons in a GaAs/AlGaAs superlattice. To produce a controllable splitting of the exciton fine-structure sublevels, we used an external magnetic field aligned differently with respect to the heterostructure growth axis. We have detected oscillations of the PL intensity, which are related to quantum beats between the split sublevels. By measuring the oscillation period, we have

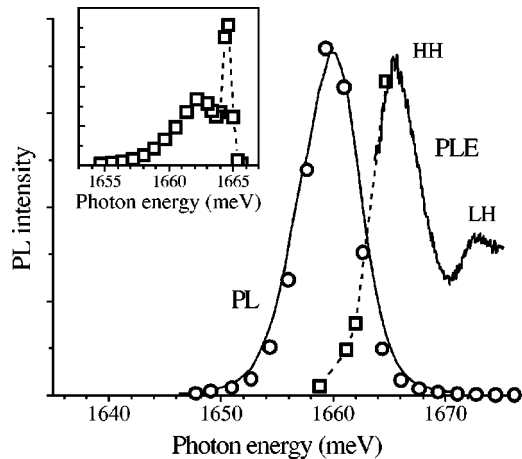


FIG. 1. PL and PLE spectra of the heterostructure under study. Solid lines are the results of cw experiments. Open circles and squares represent the data obtained by integrating the PL kinetics at selected spectral points. Inset: Integrated PL spectrum under pulsed resonant excitation (squares). Dashed line is a guide to the eye.

determined the relevant splittings and studied their dependence on strength and direction of the magnetic field. Based on the analysis of the experimental data thus obtained we have reconstructed the whole picture of Zeeman splitting of the excitonic states and have determined polarization characteristics of each Zeeman sublevel. This has allowed us to examine separately the processes of phase and energy relaxation of the exciton spin states in the structure under study. As a result, we have found the rates of each of the relaxation processes and have studied dependence of these rates on the strength and orientation of the external magnetic field.

II. EXPERIMENTAL RESULTS

A. Technical details

The studied heterostructure was grown by the molecular beam epitaxy (MBE) technique with no growth interruption on the interfaces. The structure comprised 50 periods of a superlattice with the GaAs and $\text{Ga}_{0.56}\text{Al}_{0.44}\text{As}$ layers 30 and 38 Å thick, respectively. The photoluminescence (PL) and photoluminescence excitation (PLE) spectra of the sample measured at 4.2 K both under cw and pulsed excitations are presented in Fig. 1. The excitonic PL linewidth is 6 meV, while the Stokes shift between the absorption and PL peaks is about 5 meV. These quantities well correspond to standard parameters of heterostructures with these dimensional characteristics.^{10,11}

The photoluminescence was excited by a tunable Ti:sapphire laser with the pulsewidth 3–5 ps and was detected using a Synchroscan streak camera with the time resolution 2–5 ps. The measurements were made under conditions when the PL kinetics did not depend on power density of the exciting light. The peak concentration of excitons in the sample did not exceed 10^9 cm^{-2} . Most experiments have been made at a sample temperature of 5 K.

The external magnetic field of 0–5 T was produced by a split superconducting magnet, which allowed us to make

measurements both in the Faraday and Voigt configurations. In all experiments, the magnetic field vector and exciting laser beam were arranged in the horizontal plane. The angle α between the magnetic field direction and the growth axis of the structure was varied by rotating the sample around the vertical axis. The PL of the sample was collected in a relatively small solid angle ($\approx 20^\circ$) in the back scattering geometry.

When detecting the resonant PL, special measures were taken to minimize the scattered laser light hitting the photo-detector. For the measurements, we have chosen a sample with the highest PL brightness. The superlattice contained a large number of periods, which resulted in strong absorption of the excited light. The sample had a high-quality mirror surface which made it possible to essentially reduce the scattered light intensity. The reflected laser beam was shielded by an opaque mask in the plane of the aperture diaphragm. As a result, the PL signal could be reliably detected on the background of the exciting laser pulse even under strictly resonant conditions and could be unambiguously selected by an appropriate mathematical processing. The PL spectrum reconstructed from the kinetic data is shown in the inset of Fig. 1. One can see a pronounced peak of the resonant PL on the background of the inhomogeneously broadened band excited due to spectral diffusion.

B. Kinetics of the polarized PL in zero magnetic field

The PL kinetics in the linear and circular polarizations is shown in Fig. 2. As seen from Fig. 2(a), the copolarized resonant PL builds up during the pump pulse whereas the PL pulses in cross polarizations show sloping front edges. The pulses of the Stokes-shifted PL reveal a slower rise time both in linear and circular polarizations [see Fig. 2(b)], which is related to spectral diffusion of excitations over the inhomogeneously broadened exciton line. Note that the difference between the rise times of the PL pulses in the copolarization and cross-polarization persists, i.e., the spectral diffusion virtually does not affect the PL polarization.

Dynamics of the degree of circular polarization of the PL ρ_σ , detected both at resonance with the excitation and at some Stokes shift is shown in the inset of Fig. 2. The degree of polarization was defined in the conventional way: $\rho = (I_1 - I_2)/(I_1 + I_2)$, where I_1 and I_2 are, respectively, copolarized and cross-polarized PL intensities. As seen, ρ_σ monotonously decays in time. Values of the decay time, t_0 , are found to be approximately the same both for circular and linear polarizations and close to the data of other authors obtained on similar structures.^{7,10,9} The interesting fact is that the decay time of polarization degree measured at the Stokes shift is larger than that measured at resonance conditions (see inset in Fig. 2). This means that the spectral diffusion results in decreasing depolarization rate. The nature of this unusual behavior will be discussed elsewhere. A detailed analysis of the decay of the polarization degree will be presented in Sec. III C.

So the sample under study, in terms of its spectral, polarization, and dynamic characteristics, is fairly typical and conclusions that can be made based on a more detailed analysis of its polarization dynamics are sufficiently general.

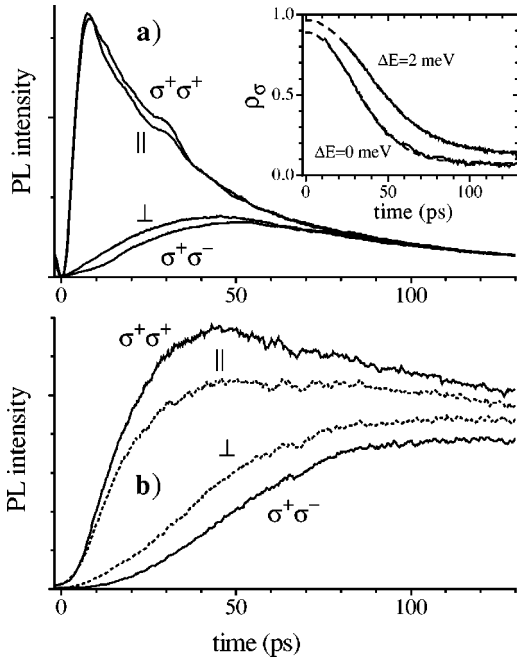


FIG. 2. The PL kinetics in different polarizations detected at resonance with the exciting light (a) and at a Stokes shift of 2 meV (b). Excitation energy is 1662 meV. The colinearly and cross-linearly polarized signals are denoted by symbols \parallel and \perp ; the co-circularly and cross-circularly polarized signals are denoted by $\sigma^+\sigma^+$ and $\sigma^+\sigma^-$, respectively. Inset: kinetics of the degree of circular polarization of the PL detected at strict resonance with the exciting light ($\Delta E=0$ meV) and with the Stokes shift $\Delta E=2$ meV. The noisy curves are the experimental results, the dashed curves are a theoretical fit by Gaussian function $\rho(t)=\rho(0)\exp[-(t/t_0)^2]$. Values of the decay time t_0 are 41 ps and 53 ps for the curves measured at Stokes shift 0 and 2 meV, respectively.

C. The PL kinetics in a magnetic field

In the measurements made in an external magnetic field, the PL was detected at the wavelength detuned from that of excitation by 2 meV toward lower energies. Such a detuning made it possible to completely get rid of the scattered laser light. At the same time, as mentioned above, this detuning did not cause any noticeable PL depolarization.

The PL kinetics in the longitudinal magnetic field, parallel to the growth axis z (Faraday geometry), is shown in Fig. 3(a). As is seen, the circularly polarized PL pulses retain smooth shape while the PL intensity in linear polarizations shows pronounced oscillations. Phases of the oscillations for the colinear and cross-linear polarizations of the PL are opposite. Figure 3(b) demonstrates dynamics of the PL polarization degree. One can see that the degree of circular polarization ρ_σ gradually decays in time while the degree of linear polarization ρ_l oscillates symmetrically with respect to the abscissa axis. The oscillations can be well approximated by the function

$$\rho(t)=\rho(0)\exp(-t/\tau)\times\cos(\omega t). \quad (1)$$

This approximation allowed us to determine the frequency and decay time of the oscillations (ω and τ , respectively). It

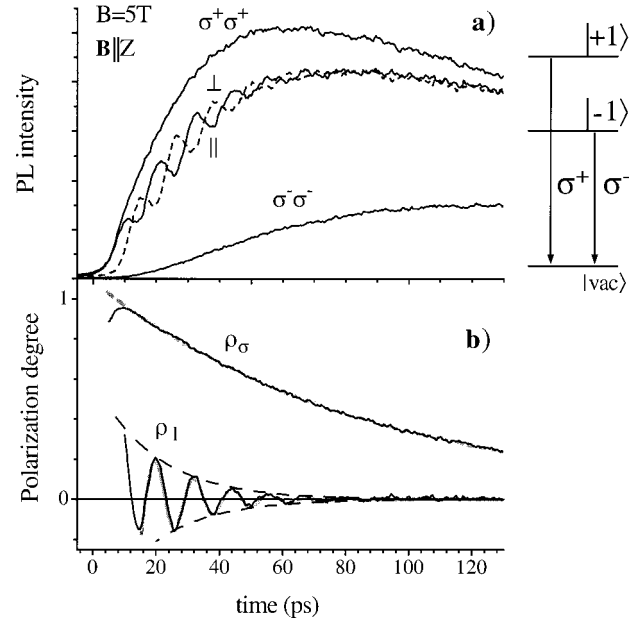


FIG. 3. (a) PL kinetics in a magnetic field $B=5$ T which is parallel to the growth axis z (Faraday geometry). PL polarizations are shown by symbols close each curve. A scheme shows optical transitions from Zeeman components of the bright excitonic state. (b) Dynamics of the degree of circular polarization ρ_σ and linear polarization ρ_l of the PL. Thick gray lines show theoretical fit of the curve ρ_l by function (1) with the parameters $\tau_l=18$ ps, $\omega_l=0.52$ ps $^{-1}$, and of the curve ρ_σ by the exponential function $y=y_0\exp(-t/t_0)$ with $t_0=85$ ps. Dashed curves show decay of the oscillations in ρ_l fitted by functions $y=\pm y_0\exp(-t/\tau)$.

has been shown experimentally that the frequency of the oscillations in linear polarization ω_l grows linearly with the magnetic field strength.

Unlike the longitudinal magnetic field, the transverse magnetic field directed perpendicular to the z axis (Voigt geometry) causes pronounced PL intensity oscillations in the circular right and left copolarizations ($\sigma^+\sigma^+$ or $\sigma^-\sigma^-$). An example of the oscillating kinetics is shown in Fig. 4(a) (curve 1). The oscillating part of the PL normalized to the envelope amplitude I_{beats} can be well approximated by function (1) as shown in Fig. 4(b). In the cross polarizations ($\sigma^+\sigma^-$ or $\sigma^-\sigma^+$), no oscillations are observed [see curve 2 in Fig. 4(a)]. A decrease in the transverse magnetic field is accompanied by abrupt (approximately quadratic) drop of the oscillation amplitude (see inset in Fig. 4). Under linearly polarized excitation, the oscillations in the transverse magnetic field are virtually absent.

Dynamics of the polarized PL in magnetic fields tilted at an angle α to the growth axis is characterized by the following features. Oscillations in the degree of linear polarization persist, but their frequency decreases with the angle α (see Fig. 5). Analysis of the data has shown that the main characteristics of the oscillations (frequency and decay constant) obtained in the tilted magnetic field B totally coincide with those in the longitudinal field $B_z=B\cos\alpha$. It follows herefrom that dynamics of the degree of linear polarization is controlled exclusively by longitudinal component of the magnetic field.

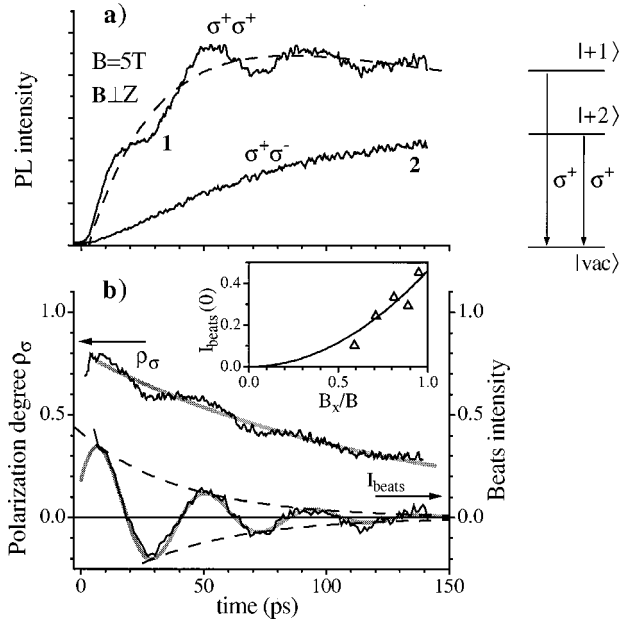


FIG. 4. (a) PL kinetics in $\sigma^+\sigma^+$ and $\sigma^+\sigma^-$ polarizations in transverse magnetic field $B=5$ T (Voigt geometry). Dashed curve shows the nonoscillating part of the signal (envelope function) approximated by $y=y_0[\exp(-t/\tau_{PL})-\exp(-t/\tau_r)]$ with $\tau_{PL}=44$ ps, $\tau_r=28$ ps. A scheme shows transitions from the “bright” and “dark” excitonic states in the transverse magnetic field which are responsible for the observed oscillations (see further details in Sec. III B 3). (b) Upper curves show the degree of circular polarization ρ_σ (noisy curve) and its fit by exponential function $y=y_0 \exp(-t/t_0)$ with $t_0=125$ ps (thick gray curve). Lower curves show the oscillating part of the PL kinetics (noisy curve) and the fit by Eq. (1) (thick gray curve) with parameters $\tau_\sigma=44$ ps, $\omega_\sigma=0.14$ ps $^{-1}$. Dashed curves show decay of the oscillations fitted by functions $y=\pm y_0 \exp(-t/\tau_\sigma)$. Inset: dependence of the QB amplitude on transverse component of the magnetic field. Solid line is the fit of experimental data (triangles) by function $y=ax^2$.

The circularly polarized PL pulses retain smooth shape upon deviation of the magnetic field from the longitudinal direction up to the angle $\alpha \approx 30^\circ$. At higher angles α , however, the circularly polarized PL starts to show oscillations similar to those observed in the transverse field. The oscillation amplitude strongly increases with increasing α , i.e., with increasing transverse component of the magnetic field. It is important that the oscillation frequencies in the $\sigma^+\sigma^+$ and $\sigma^-\sigma^-$ polarizations are essentially different. The frequency difference decreases with increasing α as shown in Fig. 6 and, in the exactly transverse field, the oscillation frequencies in the $\sigma^+\sigma^+$ and $\sigma^-\sigma^-$ polarizations appear to be equal.

D. Relaxation characteristics of the polarized PL

The exciton spin dynamics is revealed experimentally in three independent types of relaxation processes. The first process is relaxation of the degree of circular polarization of the PL ρ_σ . Dynamics of ρ_σ in the absence of magnetic field is shown in the inset of Fig. 2(a). We found that the time dependence of ρ_σ can be better approximated by the Gauss-

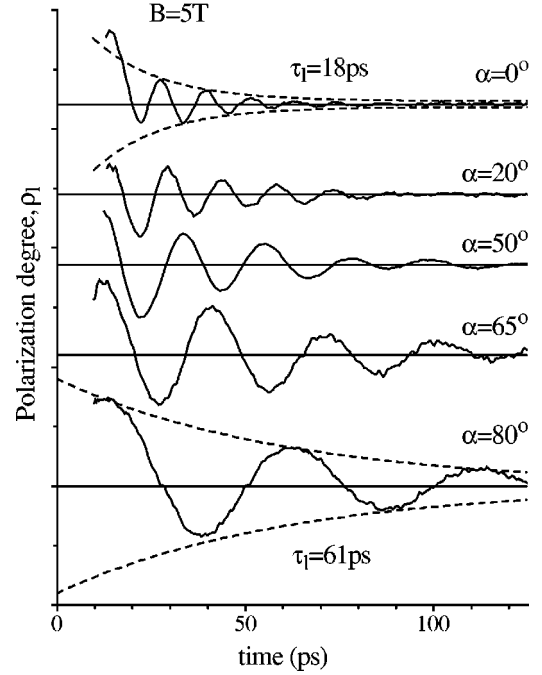


FIG. 5. Degree of linear polarization, ρ_l , at different angles α between the magnetic field direction and z axis of the sample. The angle is indicated close each curve. The dashed lines are the fit of ρ_l by the envelope functions $y=\pm y_0 \exp(-t/\tau_l)$ with the indicated values of decay time τ_l .

ian $\rho(t)=\rho(0)\exp[-(t/t_0)^2]$ rather than by an exponential function. The decay time t_0 is close to 40 ps for strictly resonant PL and increases with increasing detuning from the resonance.

In the presence of a longitudinal magnetic field, the decay of ρ_σ is modified and becomes to be purely exponential in high magnetic fields [see Fig. 3(b)]. The decay time t_0 strongly depends on the magnetic field strength B . An increase of B from 0 to 1 T is accompanied by approximately threefold increase of t_0 , while further increase of B does not affect the value t_0 .

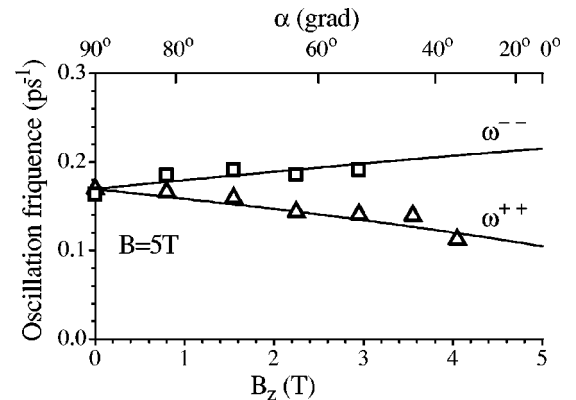


FIG. 6. Angular dependence of the oscillation frequency of the circularly copolarized PL under the right- (ω^{++}) and left- (ω^{--}) circularly polarized excitation. Solid lines are the theoretical fits as described in Sec. III B.

In the transverse and tilted magnetic field, time dependence of ρ_σ consists of a smooth component and an oscillating one [see Fig. 4(b)]. Decay time of the smooth component, t_0 , is found to be independent of the transverse component of the magnetic field B_x , but strongly sensitive to the longitudinal field B_z . Appearance of even small longitudinal component upon deviation of the magnetic field from the transverse direction is accompanied by an essential increase of the decay time t_0 . The experiments performed in the tilted magnetic field have shown that the dependence of t_0 on the tilt angle α is totally determined by variations of B_z .

The second relaxation process is the decay of the oscillations observed in the degree of linear polarization, ρ_l (see Fig. 3). We studied dependence of dynamics of ρ_l on the magnetic field B . The transverse component B_x , as mentioned above, does not affect the dynamics of ρ_l . For this reason we varied the longitudinal component B_z by two ways: either by changing the value of the longitudinal magnetic field (keeping $\alpha=0^\circ$) or by changing the tilt angle α at a fixed value of B . Variations of the ρ_l dynamics with the angle α presented in Fig. 5 shows that a decrease of α and, hence, an increase of B_z is accompanied by essential shortening of the decay time of the oscillations.

Finally, the third relaxation process is the decay of the oscillations of the circularly polarized PL I_{beats} observed in the transverse [see Fig. 4(b)] and tilted magnetic fields. It was found that the oscillation decay time is essentially independent either of the strength or of the tilt angle of the magnetic field and equals $\tau_\sigma=(50\pm 10)$ ps.

III. ANALYSIS OF THE RESULTS

To identify adequately the relaxation processes, whose parameters were discussed in the previous section, one has to know exactly which particular states are involved into the observed optical transitions. For this reason, we start with

analysis of behavior of the fine-structure sublevels in magnetic field.

A. Fine structure of the excitonic states

Fine structure of the HH exciton is formed by four basis states, $|\pm 1\rangle$ and $|\pm 2\rangle$, corresponding to projections of the total angular momentum on the quantization axis $J_z=J_{hz}-S_e=\pm 1$ and $J_z=J_{hz}+S_e=\pm 2$ where J_{hz} is the projection of the hole angular momentum and S_e is the electron spin. To analyze the fine structure, we will use the effective Hamiltonian $H=H_{\text{exc}}+H_{\text{Zeeman}}$ given in Ref. 12. The Hamiltonian accounts for the exchange interaction between the electron and hole

$$H_{\text{exc}} = \sum_{i=x,y,z} (a_i J_{h,i} S_{e,i} + b_i J_{h,i}^3 S_{e,i}) \quad (2)$$

and Zeeman splitting in the magnetic field B

$$H_{\text{Zeeman}} = \mu_B \sum_{i=x,y,z} \left(g_{e,i} S_{e,i} - \frac{g_{h,i}}{3} J_{h,i} \right) B_i, \quad (3)$$

where a_i and b_i are the constants of the exchange interaction and $g_{e,i}$ and $g_{h,i}$ are the electron and hole g factors, respectively.

Using the basis functions $|+1\rangle$, $|-1\rangle$, $|+2\rangle$, and $|-2\rangle$, the spin-Hamiltonian can be represented as a 4×4 matrix with its elements containing the electron-hole exchange interaction energies and Zeeman energies of the levels. The Hamiltonian can be essentially simplified if we take into account a strong anisotropy of the hole g factor¹² and a small anisotropy of the electron g factor,¹³ assuming $g_{h,x}=g_{h,y}\approx 0$, $g_{h,z}=g_h$, and $g_{e,x}\approx g_{e,y}\approx g_{e,z}=g_e$. In addition, we will neglect anisotropic component of the exchange interaction bearing in mind that the latter is small compared with the energy of the isotropic exchange.¹⁴ Within these approximations, the spin-Hamiltonian matrix gains the form

$$H = \frac{1}{2} \begin{pmatrix} \delta + g_{\pm 1} \mu_B B \cos \alpha & 0 & g_e \mu_B B \sin \alpha & 0 \\ 0 & \delta - g_{\pm 1} \mu_B B \cos \alpha & 0 & g_e \mu_B B \sin \alpha \\ g_e \mu_B B \sin \alpha & 0 & -\delta - g_{\pm 2} \mu_B B \cos \alpha & 0 \\ 0 & g_e \mu_B B \sin \alpha & 0 & -\delta + g_{\pm 2} \mu_B B \cos \alpha \end{pmatrix}, \quad (4)$$

where $g_{\pm 1}=g_e+g_h$ and $g_{\pm 2}=g_e-g_h$, δ is the energy of the isotropic exchange determined by H_{exc} , μ_B is the Bohr magneton, and α is the angle between the magnetic field direction and z axis.

The fairly simple form of the spin-Hamiltonian allows us to obtain analytical expressions for the energy eigenvalues E_i of components of the fine excitonic structure in a magnetic field of arbitrary orientation by solving the stationary Schrödinger equation $H\Psi_i=E_i\Psi_i$, for the eigenfunctions Ψ_i expressed through linear combinations of the basis functions.

The obtained equations for eigenvalues and eigenfunctions are presented in Table I.

Equations for the coefficients c_{ij} at arbitrary orientation of the magnetic field are rather cumbersome and, for this reason, are not given in the table. In the absence of the magnetic field ($B=0$) the quantities E_i have only two different values $E_1=E_2=\delta/2$ and $E_3=E_4=-\delta/2$ (see Table I), i.e., the fine structure of the HH exciton is split by the exchange interaction into two degenerate doublets with optical transition into one of them ($J_z=\pm 1$) being allowed and into the other

TABLE I. Excitonic states in a magnetic field.

i	E_i	Ψ_i
1	$+\frac{1}{2}[(g_h\mu_B B \cos \alpha) + \sqrt{(\delta + g_e\mu_B B \cos \alpha)^2 + (g_e\mu_B B \sin \alpha)^2}]$	$c_{11} +1\rangle + c_{13} +2\rangle$
2	$-\frac{1}{2}[(g_h\mu_B B \cos \alpha) - \sqrt{(\delta - g_e\mu_B B \cos \alpha)^2 + (g_e\mu_B B \sin \alpha)^2}]$	$c_{22} -1\rangle + c_{24} -2\rangle$
3	$+\frac{1}{2}[(g_h\mu_B B \cos \alpha) - \sqrt{(\delta + g_e\mu_B B \cos \alpha)^2 + (g_e\mu_B B \sin \alpha)^2}]$	$c_{31} +1\rangle + c_{33} +2\rangle$
4	$-\frac{1}{2}[(g_h\mu_B B \cos \alpha) + \sqrt{(\delta - g_e\mu_B B \cos \alpha)^2 + (g_e\mu_B B \sin \alpha)^2}]$	$c_{42} -1\rangle + c_{44} -2\rangle$

($J_z = \pm 2$) forbidden by the selection rules in total angular momentum.

In the longitudinal magnetic field ($\alpha=0$), the equations for the energy eigenvalues acquire the form

$$E_{1,2} = 1/2[\delta \pm \mu_B B(g_h + g_e)],$$

$$E_{3,4} = 1/2[-\delta \pm \mu_B B(g_h - g_e)]. \quad (5)$$

It follows from Eqs. (5) that each of the doublets splits and the splitting energies $\Delta_{12} = E_1 - E_2$ and $\Delta_{34} = E_3 - E_4$, are linearly related to the magnetic field strength. Note that the ratio of the splittings of the dark and bright doublets depends on the electron g -factor sign, which can be either positive or negative depending on the values of parameters of the structure.^{15,22}

The transverse magnetic field ($\alpha=90^\circ$) does not lift the degeneracy of the doublets but changes the distance between them:

$$\Delta_{13} = E_1 - E_3 = \sqrt{\delta^2 + (g_e\mu_B B)^2} = \Delta_{24}. \quad (6)$$

It is evident that the energy gap between the dark and bright doublets is determined by geometrical sum of the exchange and Zeeman splitting. Thus, in comparatively small magnetic fields, when $g_e\mu_B B \ll \delta$, the gap between the doublets is virtually insensitive to the field strength.

In the tilted magnetic field, the splitting of the fine structure is determined by combined action of the longitudinal and transverse components of the field. As was pointed out above, in the relatively small magnetic fields, when $g_e\mu_B B/\delta \ll 1$, the transverse component virtually does not affect the energy of the state. In this case, the equations for the eigenvalues E_i will practically coincide with Eqs. (5) if we use the value of the longitudinal component $B_z = B \cos \alpha$ as the field strength.

B. Quantum beats

The analysis performed above allows us to make clear specific features of dynamics of the polarized PL in magnetic field. We discuss the PL dynamics for different orientations of the magnetic field separately.

1. Longitudinal magnetic field

In the longitudinal magnetic field ($B=B_z$), the Hamiltonian remains diagonal and the basis functions are not mixed. The magnetic field splits the bright doublet ($J_z = \pm 1$) into two states. Transitions from these states correspond

to the right and left circularly polarized oscillators. The optically inactive (dark) doublet is split into the states $|+2\rangle$ and $|-2\rangle$ with transitions into them remaining forbidden.

Circularly polarized light excites only one component of the bright doublet, while the linearly polarized light excites both components creating a coherent superposition of the right- and left-polarized oscillators. Total emission of such oscillators, which are split by the energy Δ_{12} (see Sec. III A), can be represented as a linearly polarized emission with its polarization plane rotating with the frequency $\omega_l = \Delta_{12}/\hbar$. This rotation is revealed experimentally as antiphase oscillations (quantum beats) of the PL intensity in two orthogonal linear polarizations. The dynamics of the linearly polarized PL in the longitudinal magnetic field observed experimentally (see Fig. 3) perfectly correlates with the above model.

By measuring the beat frequency ω_l one can directly determine the value of the Zeeman splitting of the optically active doublet Δ_{12} . As was shown experimentally, the splitting is a linear function of the magnetic field strength. This makes it possible to determine the g factor of the optically active excitonic state $g_{\pm 1} = (g_h + g_e) = \Delta_{12}/\mu_B B = -1.13 \pm 0.05$. We consider $g_{\pm 1}$ to be negative according to the negative value of g_h (Ref. 12) and also taking into account that $|g_e| < |g_h|$.⁷

2. Transverse magnetic field

Transverse magnetic field does not lift degeneracy of the bright states. Therefore, in this case, no quantum beats like those detected in longitudinal magnetic field can be observed. At the same time, the transverse field mixes the bright and dark states that partially allows optical transitions into the dark doublet. Appearance of the transitions from the optically inactive states in the transverse magnetic field was observed experimentally in the PL spectra of single quantum dots in Ref. 16.

As follows from the equations listed in Table I, the transverse magnetic field mixes the state $|+1\rangle$ with the state $|+2\rangle$ and $|-1\rangle$ with $|-2\rangle$. As a result, the right circularly polarized (σ^+) light simultaneously excites not only the state $|+1\rangle$, but also the state $|+2\rangle$, spaced from the former by the energy Δ_{13} . This should give rise to quantum beats revealed in the copolarized PL intensity ($\sigma^+ \sigma^+$) at a frequency of $\omega = \Delta_{13}/\hbar$. It is exactly what we observe experimentally (see Fig. 4).

Under the left circularly polarized excitation (σ^-), quantum beats arise on transitions from the states $|-1\rangle$ and $|-2\rangle$ and are observed in the $\sigma^- \sigma^-$ co-polarized PL. Since the

splittings Δ_{13} and Δ_{24} are the same in the transverse magnetic field [see Eqs. (6)], the beat frequencies in the $\sigma^+\sigma^+$ and $\sigma^-\sigma^-$ polarizations are equal too.

Dipole moments of the transitions from the dark states are controlled by the coefficients c_{ik} (see Table I). In small magnetic field, c_{ik} are proportional to the transverse component of the magnetic field. In this case, the beat amplitude, which is proportional to the dipole moment squared of these transitions¹⁷ should quadratically depend on the strength of the transverse magnetic field. This conclusion also well agrees with the experimental data discussed above [see inset in Fig. 4(b)].

The cross-polarized PL arises only after energy relaxation of the spin states that destroys the coherence created by the light and thus inhibits appearance of the quantum beats. This explains behavior of the cross-polarized PL kinetics shown in Fig. 4(a).

Analysis of dependence of the oscillation frequency on the transverse magnetic field makes it possible, in principle, to determine the value of the electron g factor using Eqs. (6). As has been shown experimentally, however, the beat frequency remains virtually the same up to the field of $B = 5$ T. In conformity with the conclusions made in the previous section, it means that the electron Zeeman splitting is much smaller in these magnetic fields than the exchange energy $g_e\mu_B B \ll \delta$, i.e., the electron g factor is too small to be measured in this experiment.

3. Tilted magnetic field

In the tilted magnetic field, the polarized PL dynamics is affected both by the longitudinal and transverse components of the magnetic field but the roles of these components are essentially different. The transverse component mixes the bright and dark excitonic states but virtually does not affect their energy structure. The longitudinal component, on the contrary, totally controls the values of the Zeeman splittings and does not affect the mixing of the states. Based on this, it is not difficult to analyze the results obtained in the tilted magnetic fields.

Dynamics of the linearly polarized PL is controlled mainly by quantum beats between the bright doublet components since transitions from these components are the strongest. The beat frequency is determined in this case by longitudinal component of the magnetic field $B_z = B \cos \alpha$. This conclusion well agrees with the experimental data presented in Sec. II C and allows us to determine the value of the exciton g factor $g_{\pm 1}$ with high accuracy by measuring the beat frequency in dependence on the tilt angle α at a fixed strength of the magnetic field. The value $g_{\pm 1}$ given above is obtained with allowance for these data.

A specific feature of the beats in the circularly polarized PL is that their amplitude is given by transverse component of the magnetic field while their frequency depends on the longitudinal component. Using equations listed in Table I, one can notice that the energy difference $E_1 - E_3$ should decrease with increasing longitudinal component, while the difference $E_2 - E_4$ should grow. In accordance with this behavior, the beat frequencies in the $\sigma^+\sigma^+$ and $\sigma^-\sigma^-$ polarizations should differ in the tilted magnetic field. This

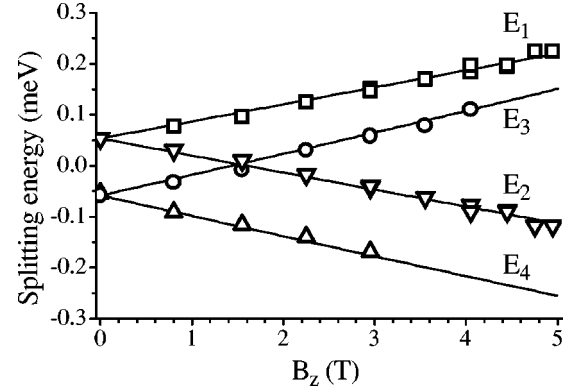


FIG. 7. Zeeman splitting of the bright and dark exciton doublets in a longitudinal magnetic field. The results of processing the experimental data using the procedure described in the text are shown by symbols. Solid lines are the results of calculation by the formulas given in Table I with the values of the parameters $g_e = 0.12$, $g_h = -1.25$, and $\delta = 0.106$ meV.

conclusion well correlates with the experimental data shown in Fig. 6. As seen, the beat frequencies in the $\sigma^+\sigma^+$ and $\sigma^-\sigma^-$ polarizations are noticeably different, with the difference being higher for smaller tilt angles, i.e., for larger longitudinal components of the magnetic fields.

Theoretical fit of the experimental data presented in Fig. 6 by the formulas from Table I allows us to determine the values of the exchange splitting, $\delta = 0.106 \pm 0.01$ meV, and electron g factor $g_e = 0.12 \pm 0.01$. Zeeman splitting in the magnetic field $B = 5$ T corresponding to the found value of g_e approximately equals 0.03 meV. This splitting is really essentially smaller than the exchange splitting. Thus, the above approximation $g_e\mu_B B \ll \delta$ can be considered to be well justified.

In our experiments, we did not determine sign of the electron g factor. Based on the data presented in Ref. 13, we suppose that g_e is positive. Using these data, one can find the hole g factor $g_h = g_{\pm 1} - g_e = -1.25 \pm 0.06$.

4. Fine structure

The analysis of the quantum beats performed above has allowed us to construct the whole picture of the Zeeman splitting in the structure under study shown in Fig. 7. The splitting of the optically active doublet in the magnetic field was obtained based on the experimental beat frequencies ω_l in linear polarizations using the formula $E_{1,2} = 1/2(\delta \pm \hbar \omega_l)$. To plot splitting of the dark doublet we used the beat frequencies in circular polarizations ω^{++} and ω^{--} shown in Fig. 6. The energies of the doublet components were determined using the formulas $E_3 = E_1 - \hbar \omega^{++}$ and $E_4 = E_2 - \hbar \omega^{--}$. Theoretical curves in Fig. 7 are fittings of the experimental data using the formulas listed in Table I. The energy diagram of the fine-structure level splitting thus obtained is used in the next section to analyze the relaxation processes.

C. Spin dynamics

Relaxation processes in spin subsystems can be divided into two groups. The first one includes the processes of en-

ergy relaxation accompanied by changes of the spin sublevel populations. Dynamic characteristic of these processes is the lifetime T_1 . The second group includes phase relaxation processes, which conserve populations of spin states but destroy their coherence. This processes are characterized by the dephasing time T_2 . In this subsection, we separately discuss each of these processes.

1. Energy relaxation of spins

In the absence of the magnetic field, depolarization dynamics of the excitonic emission is controlled by two processes: by relaxation into nonradiative states $J_z = \pm 2$ and by relaxation between the optically active sublevels $J_z = \pm 1$. Analysis of the rate equations performed in Ref. 18 shows that the first process should lead to a pronounced nonexponentiality of the total (in both polarizations) PL intensity. In our case, however, the resonant PL decay can be well approximated by a single-exponential function within the time interval 0–300 ps.¹⁹ Therefore, we can conclude that the process of relaxation into the nonradiative states is inefficient. This conclusion agrees well with the data of Ref. 20, where an efficient relaxation into the dark states was observed only under certain conditions: under interband excitation or at a sufficiently high exciton concentration.

In the absence of relaxation into the dark states, the only process that can cause depolarization of the excitonic PL is the relaxation inside the optically active doublet. The best conditions for studying this process are realized when the bright states are split and can be distinguished by choosing properly polarization characteristics of the exciting light. From this point of view, the simplest are the experiments in a longitudinal magnetic field which splits the optically active doublet into two sublevels (E_1 and E_2 in Fig. 7) leaving transitions into the dark states forbidden.

Circularly polarized light excites only one state of the doublet, and observation of the PL in the cross-polarized light is possible only after energy relaxation of the exciton spin states. It is this relaxation time, T_1 , that should determine the experimental decay rate of the degree of circular polarization of the PL in the longitudinal magnetic field, i.e., $t_0^{-1} = T_1^{-1}$. Figure 8 shows dependence of the relaxation rate t_0^{-1} on longitudinal component of the magnetic field. As seen from the figure, the relaxation rate virtually does not depend on magnetic field at $B > 1$ T and equals the value $t_0^{-1} \approx 1 \times 10^{10} \text{ s}^{-1}$. According to the aforesaid, this value should be ascribed to the energy relaxation rate between sublevels of the optically active exciton state split by the magnetic field.

The mechanism of energy relaxation of the exciton spin states calls for further investigation. The fact that the relaxation rate t_0^{-1} is independent of magnetic field for $B = (1 - 5)$ T does not allow us to attribute this value to the process of direct spin-phonon relaxation whose probability should essentially increase with increasing Zeeman splitting. Most likely, the energy relaxation is related either to the Raman spin-phonon process or to interaction with impurity spins discussed in Ref. 21.

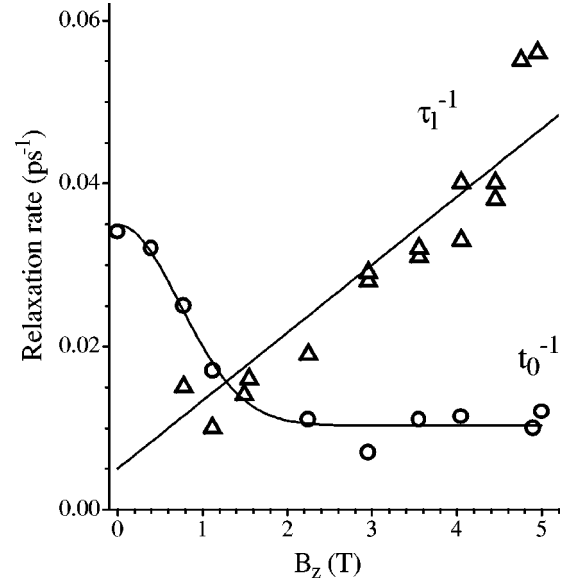


FIG. 8. Dependence of the relaxation characteristics of the polarized PL on the longitudinal field strength. Circles represent the relaxation rate for the degree of circular polarization t_0^{-1} and triangles represent the decay rate of the beats in linear polarization τ_1^{-1} . Solid lines (Gaussian over the circles and linear dependence over the triangles) are guides to the eye.

2. Phase relaxation of spins in longitudinal magnetic field

The linearly polarized light, in contrast to the circularly polarized, excites a coherent superposition of both bright doublet states. As discussed above (see Sec. III B), this gives rise to quantum beats in the polarized PL. The decay of the beats is related to destruction of the coherence, with the decay constant given by equation

$$\tau_1^{-1} = (2T_1)^{-1} + T_2^{-1}, \quad (7)$$

where T_2 is the dephasing time of the exciton spin states.¹⁸ Dependence of the beat decay rate τ_1^{-1} on the field strength, measured experimentally, is shown in Fig. 8. It is seen that the field dependencies of the quantities t_0^{-1} and τ_1^{-1} drastically differ. In the magnetic field $B > 1$ T, decay rate t_0^{-1} remains virtually constant whereas the beat decay rate τ_1^{-1} rapidly grows with the field and exceeds t_0^{-1} approximately by a factor of 5 at $B = 5$ T. Therefore, we can conclude that the relation $T_2^{-1} \gg T_1^{-1}$ is fulfilled in high magnetic field, i.e., the main mechanism of the coherence decay is the phase, rather than the energy, relaxation of the exciton spin states.

This result disagrees with conclusions of Ref. 7, where the beats between Zeeman components of the excitonic line, in a similar structure, were observed in dynamics of the induced birefringence. The authors of Ref. 7 argue that the beat decay is caused by the energy relaxation of angular momentum. The growth in the decay rate with increasing magnetic field, similar to that shown in Fig. 8, is interpreted by them as a result of growing probability of spin-phonon relaxation between Zeeman sublevels. The direct measurements of the energy relaxation rate in a magnetic field, performed in the present paper, rule out this interpretation and allow us to

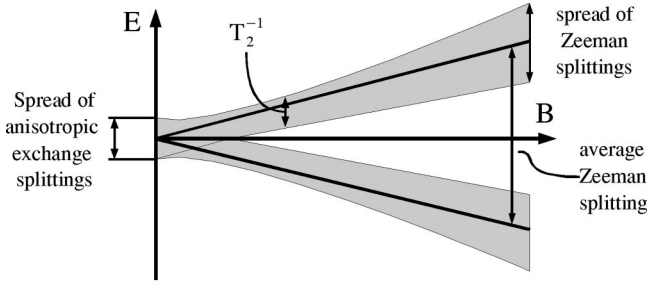


FIG. 9. A scheme of the inhomogeneous splitting of the “bright” excitonic doublet in the longitudinal magnetic field.

make a conclusion about predominant role of dephasing in decay of the quantum beats between Zeeman sublevels.

Using the obtained data, we can make certain conclusions about nature of this phase relaxation process. At low temperatures and low excitation densities, the irreversible dephasing of the exciton spin states seems to be inefficient. Most likely, the dephasing is reversible, namely, it is related to a spread of the oscillation frequencies ω_l in the inhomogeneous excitonic ensemble. The almost linear dependence of τ_l^{-1} on the field strength (see Fig. 8) counts in favor of the fact that the main reason for this spread is a local variation of the exciton g factor ($g_{\pm 1}$) giving rise to a spread of the relevant Zeeman splittings as schematically shown in Fig. 9. The spread of the splittings evaluated from the decay rate corresponds to 10% spread of the value of $g_{\pm 1}$.

3. Phase relaxation of spins in transverse magnetic field

The transverse field, unlike the longitudinal one, does not split the optically active doublet and does not affect the decay rate of the circularly polarized PL. At the same time, the experiments in the transverse field has allowed us to determine one more relaxation constant—the decay rate of oscillations in the circularly polarized PL (τ_{σ}^{-1}). The experimental results have shown that this value is $\tau_{\sigma}^{-1} = (2 \pm 0.3) \times 10^{10} \text{ s}^{-1}$ and virtually does not depend on the field strength. Since the nature of the oscillations is connected with quantum beats between the bright and dark excitonic states, their decay is caused by destruction of coherence of these states due to processes of energy and phase relaxation. It was already mentioned before, that the energy relaxation between the states $J_z = 1$ and $J_z = 2$ is inefficient. Therefore, we should assume that the main reason for decay of the oscillations is dephasing. As in the case of longitudinal field, the dephasing is most probably to be reversible, but now it is caused by random spread of the exchange interaction energies, governing the splitting between the states $J_z = 1$ and $J_z = 2$. The measured value of the decay rate corresponds to an energy spread of about $20 \text{ } \mu\text{eV}$, i.e., of about 20% of the exchange energy.

4. Specific features of spin relaxation in small magnetic field

Special attention should be given to the significant increase of the relaxation rate t_0^{-1} in the field below 1 T (see Fig. 8). In opinion of the authors of Ref. 7, where a similar effect was observed, this can be caused by an increase of the

energy relaxation rate in small fields due to overlap of Zeeman sublevels, broadened by the exciton radiative decay. The authors, however, do not specify what particular physical process related to the broadening can lead to the increase of the relaxation rate.

We suppose that the increase of t_0^{-1} in small magnetic field should be attributed to a small in-plane anisotropy of the electron-hole exchange interaction in the system under study. Such an anisotropy should cause splitting of the optically-active doublet into two states, each of them being a linear combination of the states $J_z = +1$ and $J_z = -1$. Polarization characteristics of such states correspond to two orthogonal linear oscillators lying in the plane of the layers.²² The quantum beats related to the anisotropic splitting have really been observed in the type II GaAs/AlAs superlattices.³ Since the main reason for the anisotropy is nonuniformity of interfaces, both the value of the splitting and orientation of the oscillators in the plane of the layers are of random nature. A spread of the anisotropic exchange splittings is schematically shown on the left side of Fig. 9. The circularly polarized excitation creates a coherent superposition of the split excitonic states, which decays via the reversible dephasing resulted from the spread of the splittings.²³

This assumption is confirmed, first of all, by the noted in Sec. II B Gaussian shape of the decay curve of the degree of circular polarization of the PL in the absence of magnetic field [see Fig. 2(b)]. It is exactly this shape that should be displayed by the decay in the case of reversible dephasing. The value of the depolarization rate $\tau^{-1} = (3 \pm 0.5) \times 10^{10} \text{ s}^{-1}$ given in Sec. II B corresponds to the mean value of the spread of the anisotropic splittings about $30 \text{ } \mu\text{eV}$ which is comparable with the experimentally measured values of the splittings in the type-II superlattices.³

This model also explains the effect of a longitudinal magnetic field on the decay dynamics. Zeeman splitting of the states $J_z = +1$ and $J_z = -1$ suppresses the anisotropic splittings and, thus, reduces the reversible dephasing rate. As a result, the only mechanism of circular polarization decay remaining in high magnetic fields is related to the energy spin relaxation. In these conditions, kinetics of the decay should become pure exponential, which is observed experimentally [see Fig. 3(b)].

As is seen from Fig. 8, to noticeably reduce the decay rate, it is enough to apply a longitudinal magnetic field of about 0.5 T. Such a field splits the optically active doublet by $30 \text{ } \mu\text{eV}$, i.e., by the value equal to the estimated above spread of the exchange interactions in the absence of magnetic field. This also supports the proposed model.

IV. CONCLUSION

The main experimental result of this paper is considered to be separate determination of the energy and phase relaxation times of exciton spin states in the GaAs/AlGaAs superlattice. This result was obtained based on combined analysis of the quantum beat dynamics and decay of the degree of circular polarization of the resonant PL in a longitudinal magnetic field. We have found that the energy relaxation time (the time of a real flip) of the exciton spin virtually does

not depend on the field strength and makes up, in the structure under study, 100 ps, which is close to the hole spin relaxation time in similar structures.² The dephasing rate in magnetic field appears to be much higher, with the relaxation being reversible and related to inhomogeneous spread of Zeeman splittings.

By this work, we have demonstrated efficiency of the real-time polarization and kinetic experiments for studying spin dynamics of quasi-two-dimensional semiconductor heterostructures. It became clear that to obtain reliable information about spin relaxation processes one has to use the whole amount of experimental data obtained both in the linear and circular polarizations. A crucial role is played by the external

magnetic field suppressing random splittings of the exciton fine structure resulted from nonuniformity of the interfaces in real samples. We came to a conclusion that it is exactly the reversible dephasing, caused by a spread of these splittings, rather than relaxation of individual exciton spin states, controls polarization dynamics in most experiments carried out in the absence of magnetic field.³⁻⁷

ACKNOWLEDGMENTS

The authors would like to thank Dr. V. S. Zapasskii for fruitful discussions. This work was supported by Russian Foundation of Basic Research.

*Email address: Ilya.Gerlovin@paloma.spbu.ru

¹A.P. Heberle, W.W. Ruhle, and K. Ploog, *Phys. Rev. Lett.*, **72**, 3887 (1994).

²X. Marie, T. Amand, P. Le Jeune, M. Paillard, P. Renucci, L.E. Golub, V.D. Dymnikov, and E.L. Ivchenko, *Phys. Rev. B* **60**, 5811 (1999).

³C. Gourdon and P. Lavallard, *Phys. Rev. B* **46**, 4644 (1992).

⁴S. Bar-Ad and I. Bar-Joseph, *Phys. Rev. Lett.* **68**, 349 (1992).

⁵T.C. Damen, L. Vina, J.E. Cunningham, J. Shah, and I.J. Sham, *Phys. Rev. Lett.* **67**, 3432 (1991).

⁶P. Le Jeune, X. Marie, T. Amand, F. Romstad, F. Perez, J. Barrau, and M. Brouseau, *Phys. Rev. B* **58**, 4853 (1998).

⁷R.E. Worsley, N.J. Trainor, T. Grevatt, and R.T. Harley, *Phys. Rev. Lett.* **76**, 3224 (1996).

⁸X. Marie, P. Le Jeune, T. Amand, M. Brouseau, J. Barrau, M. Paillard, and R. Planel, *Phys. Rev. Lett.* **79**, 3222 (1997).

⁹T. Amand, X. Marie, P. Le Jeune, M. Brouseau, D. Robart, J. Barrau, and R. Planel, *Phys. Rev. Lett.* **78**, 1355 (1997).

¹⁰S. Bar-Ad and I. Bar-Joseph, *Phys. Rev. Lett.* **66**, 2491 (1991).

¹¹V.F. Sapega, M. Cardona, K. Ploog, E.L. Ivchenko, and D.N. Mirlin, *Phys. Rev. B* **45**, 4320 (1992).

¹²H.W. van Kesteren, E.C. Cosman, W.A.J.A. van der Poel, and

C.T. Foxon, *Phys. Rev. B* **41**, 5283 (1990).

¹³A. Malinowski and R.T. Harley, *Phys. Rev. B* **62**, 2051 (2000).

¹⁴E. Blackwood, M.J. Snelling, R.T. Harley, S.R. Andrews, and C.T.B. Foxon, *Phys. Rev. B* **50**, 14 246 (1994).

¹⁵E.L. Ivchenko and A.A. Kiselev, *Fiz. Tekh. Poluprovodn. (S.-Peterburg)* **26**, 1471 (1992).

¹⁶M. Bayer, O. Stern, A. Kuther, and A. Forchel, *Phys. Rev. B* **61**, 7273 (2000).

¹⁷M. Dyakonov, X. Marie, T. Amand, P. Le Jeune, D. Robart, M. Brouseau, and J. Barrau, *Phys. Rev. B* **56**, 10 412 (1997).

¹⁸M.Z. Maialle, E.A. de Andrada e Silva, and I.J. Sham, *Phys. Rev. B* **47**, 15 776 (1993).

¹⁹Yu. K. Dolgikh, S. A. Eliseev, I. Ya. Gerlovin, I.V. Ignatiev, V.V. Ovsyankin, Yu. P. Efimov, I.E. Kozin, V.V. Petrov, and Y. Masumoto (unpublished).

²⁰T. Amand, D. Robart, X. Marie, M. Brouseau, P. Le Jeune, and J. Barrau, *Phys. Rev. B* **55**, 9880 (1997).

²¹L. Vina, *J. Phys.: Condens. Matter* **11**, 5929 (1999).

²²E.L. Ivchenko, *Pure Appl. Chem.* **67**, 463 (1995)

²³H. Nickolaus, H.-J. Wilsche, F. Henneberger, *Phys. Rev. Lett.* **81**, 2586 (1998).